Structural Modeling and Conformational Analysis of Aromatic Polypeptoid Models Confined to Different Environmental Conditions

Avneet Saini
Department of Biophysics
Panjab University
Chandigarh, India

ABSTRACT
Conformations of achiral and chiral aromatic homo-polypeptoids of *N*phe, *N*spe and *N*rpe were studied by quantum mechanics and molecular dynamics approaches. The amide bond geometry in model peptoids Ac-X-NMe_2 could be both cis and trans and the *N*phe peptoids adopted degenerate conformations of opposite handedness with Φ, Ψ values of ~ ± 120º, ± 150º with trans amide bond geometry. This degeneracy was lifted with increase in chain length; in favor of the structure with Φ = -120º, Ψ = -150º. Polypeptoids of *N*spe and *N*rpe with and without protecting groups populated states with Φ, Ψ values of ~ 110º, 155º & -110º, -165º respectively with trans amide bond geometry.

Simulation studies in water revealed that with protecting groups peptoid Ac-(*N*spe/*N*rpe)$_5$-NMe_2 populated with cis amide bond geometry in PP type I and inverse PP type I helices respectively due to interactions between the solvent molecules and carbonyl oxygens of the backbone. Without protecting groups these polypeptoids populated poly-L-proline type II conformations. In DMSO these peptoids were shown to populate in PP type-I and inverse PP type-I helices and without protecting groups they could be realized in PP type-I as well as inverse PP type-I conformation whereas the peptoid -*N*rpe$_6$-NH_2 could be realized in inverse PP type-I conformation. Analysis of simulation results as a function of time ruled out amide bond inter-conversions between cis and trans geometry. Hence, like polyproline peptoids can also be exploited as molecular spacers.

Keywords
biomimetic, *N*phe/*N*rpe/*N*spe peptoids, simulations, conformational analysis, PP and inverse PP structures.

1. INTRODUCTION
Oligomers of *N*-substituted glycine or peptoids are synthetic peptidomimetics with sidechains attached to the amide nitrogen; rendering the backbone achiral. Their ability to fold into discrete structures and mimic the biological functions of peptides make them attractive scaffolds for biological applications as they have enhanced proteolytic stability [1] and cellular uptake [2]. Moreover, it is possible to carry out their large-scale synthesis in a cost effective way than peptides [3]. Also, the rapid room temperature synthesis of a wide variety of *N*-aryl glycine-rich peptoid oligomers with both electron-withdrawing and donating substituents is possible in good yields through silver-mediated reactions [4]. Thus, peptoids are extensively used as peptide mimics particularly of antimicrobial peptides [5-7], antibacterial magainin peptides [8] and lung surfactant proteins [9]. Their cell penetrating properties [10] and antifouling action on surfaces [11-14] and as drug and gene delivery agents are also being exploited [15,16]. Peptoids have also been designed to mimic turn formation [17-19]. Designing peptoid biomimics is not straightforward due to lack of conformational rigidity compared to α-peptides. The nature of backbone amide nitrogen is tertiary similar to that in proline and *N*-methylated amino acid residues [20]. Molecular orbital calculations have shown that the energy difference between cis and trans forms of an imide bond in proline containing peptides is low (~ 0.5 kcal mol^{-1}) due to the almost symmetrical environment, implying that cis conformation may also be populated [21]. Such information for peptoids needs to be investigated thoroughly.

Sarcosine, the simplest peptoid with minimal steric restrictions occurs in some natural proteins and polypeptides [22], surface grafted polysarcosine can be used as antifouling polymer brushes [23]. The amide bond geometry in both unblocked and blocked poly-sarcosine peptoids[23] has been reported to be trans [24]. Peptoids are generally synthesized by coupling a haloacetic acid and a primary amine by using DMF or DMSO as solvents [25]. Due to the hydrophobic nature of peptoids compared to the corresponding amino acids they are difficult to crystallize and their structural studies have mainly been carried out by circular dichroism- a low resolution technique and NMR spectroscopy [23,26-31]. Also, crystallographic studies are mostly on cyclic peptoids and there are only a few studies on linear peptoids [32-36]. The amide bond geometry has been reported as cis in *N*-(1-cyclohexylyethyl) glycine pentamers (in this study DMSO was used as a solvent at the coupling stage and crystals grown from methanol) and trans with *N*-aryl & *N*-hydroxyl achiral sidechains (here DMF was the solvent at the coupling stage and crystals grown from CH_2Cl_2/n-hexane) [32-37]. It may also be mentioned that in poly *N*-methylated α-peptides the amide bond geometry has also been shown to be trans by crystallographic results [28,29]. A careful analysis of literature leads to an interesting observation that when peptoids were synthesized using dimethyl formamide (DMF) [31,32,34-37], or dimethyl sulphoxide (DMSO) [25,26,27] as solvents during the coupling reactions; the results obtained on amide bond geometry are at variance including crystallographic studies and hence the adopted structures. This implies that the nature of amide bond geometry is influenced by the solvents being used during peptoid synthesis at the coupling stage.

Even in peptoids comprising of 100% achiral aromatic *N*phe [*N*-(1-phenylmethyl) glycine side chains no net CD signal was displayed [28,29] but no explanation has been forwarded for this. It may be mentioned that systems having no chiral centers can also exhibit CD signal due to the formation of

well defined single handed structures [38]. Thus, it will be worth investigating whether *N*phe peptoids adopt well defined structures of opposite handedness. Also, in earlier reports conformational behavior of *N*spe and *N*rpe peptoids has been reported by CD spectroscopy [27-29] a low resolution technique and the results interpreted without the knowledge of stabilizing interactions.

Here, we report conformations of homo-polypeptoids with achiral and chiral aromatic sidechains; *N*-(1-phenylmethyl) glycine i.e. *N*phe and *N*-(1-phenylethyl) glycine i.e *N*spe and *N*rpe, with focus on: i) the nature of amide bond geometry i.e. cis or trans, ii) effect of protecting groups on the structures adopted by peptoids, iii) "do peptoids adopt 'regular' structures?", iv) the interactions stabilizing the adopted structures, v) role of chirality in side chain, and vi) effect of solvents i.e. water and DMSO on the structures adopted.

2. METHODOLOGY

Knowledge about the global, local and low energy minima of model di and tripeptoids was obtained from the Φ, Ψ maps and χ potential energy curves constructed using standard bond lengths and bond angles [39]. Energy calculations were carried out using the semi-empirical QM-PCILO (**P**ertubative **C**onfiguration **I**nteraction using **L**ocalised molecular **O**rbitals) method [40] and energy minimization was done by the systematic variation of torsion angles, keeping bond lengths and angles constant. The conformational states for polypeptoids were generated from the knowledge of the global, local and low energy minima in the Φ, Ψ maps and χ curve and their energies computed. The minimization was further refined by varying Φ, Ψ and χ values in the neighborhood of the minima so obtained in steps of 5 degree and then 2 degree steps.

Minima obtained by PCILO calculations are also the minima at *ab initio* level for usual amino acids [41] and for dehydroamino acids [42-44] PCILO results [45,46] for peptides containing usual and unusual amino acids are in conformity with *ab initio* results [47,48] and knowledge based crystallographic data [48-50].

The stable conformations predicted by QM calculations served as the starting geometries for performing molecular simulations using the GROMACS software package [51]. In our study all atoms of the system were considered explicitly. The simulation results obtained by GROMOS force field have been found to be in good agreement with the experimental results on β peptides and peptoids [26,27,52]. The Dundee-PRODRG2 server [53] was used to obtain the GROMACS topology and coordinate files. All the systems were constructed by placing the energy minimized peptoid in the centre of the simulation box maintaining a distance of 1 nm from the surface of the peptoid. The peptoid was solvated with water and simple point charge (SPC) water model was used. In order to allow equilibration of solvent around the model sequence, position of all the residues was restrained for 20 ps and MD at 300 K was carried out. The Lennard-Jones interactions are cut off at 1.0 nm. Simulations for 1ns on the *N*phe and hexa-peptoid models of *N*spe and *N*rpe were performed in water [54] and DMSO [55] and interaction parameters within the design sequence were taken from GROMOS-96 force field [56]. MD simulation for 1ns at 300 K, without any restrictions was carried out in a simple cubic periodic box under NVT conditions with a time step of 2 fs [57] using the Leap Frog Algorithm [58]. Temperature was controlled through weak coupling to a bath of constant temperature [59] using a coupling time; τ_p of 0.1ps. LINCS algorithm [60] was used to restrict all bonds to their equilibrium lengths and the center of mass motion of the system removed every step to maintain the effective simulation temperature at 300 K. Long range forces were updated every 10 fs during generation of the neighbor list. The Long Range Electrostatic Interactions were calculated using a Particle Mesh Ewald Summation [61]. Initial velocities of all atoms were taken from a Maxwellian distribution at the desired initial temperature.

3. RESULTS AND DISCUSSION

3.1 Quantum Mechanical Results

Shifting of amino acid side chain from C_α to nitrogen not only affects the backbone Φ, Ψ values but also affects the amide bond geometry. To start with, conformational behavior of model dipeptoids of the form Ac-X-NMe_2 with X= *N*phe, *N*spe, *N*rpe were studied and results summarized in Table 1. Plot of energy versus ω values for the most stable states as shown in Figure 1 clearly indicated that the amide bond geometry is cis with $\omega = 0 \pm 20°$ or trans with $\omega = 180 \pm 20°$ with an energy barrier ≥ 12 kcal mol^{-1}.

Table 1. Conformational results for dipeptoids of the type Ac-X-NMe_2

Φ, ψ, *ω* χ_i, χ_j	ΔE kcal/mol	**Φ, ψ, *ω*** χ_i, χ_j	ΔE kcal/mol
Ac-*N*phe-NMe_2			
120, 165, -178	0	**-120, -150, 0**	0
-150, -95		140, 110	
-120, -150, 178	0.7	**120, 150, 0**	0
140, 110		-140, -110	
Ac-*N*rpe-NMe_2			
-110, -165, 180	0	**90, 150, 0**	6.3
-100, 110		120, 120	
0, 90, 180	4.8	**-90, -150, 0**	3.8
-150, 120		120, 120	
0, -90, 180	4.8		
-150, -150			
Ac-*N*spe-NMe_2			
120, 150, 180	0.04	**90, 150, 0**	4.2
105, -115		-120, 120	
0, 90, 180	4.2	**-90, -150, 0**	4.6
150, 120		-120, 120	
0, -90, 180	4.0		
150, 120			

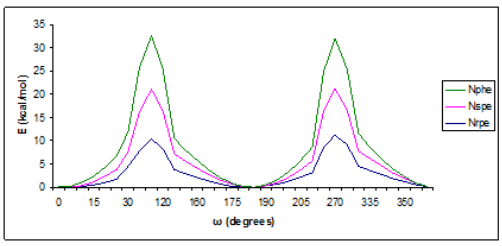

Figure 1. Plot of Energy *vs.* ω for model peptoids clearly reflects that the amide bond geometry can be both cis and trans.

Like the L and D amino acids [62,63], the peptoids Ac-*N*spe-NMe_2 and Ac-*N*rpe-NMe_2 were also found to be degenerate on the energy scale. This implies that these peptoids could be realized in both cis and trans amide bond geometry with appropriate choice of the experimental conditions during synthesis/study. Therefore, conformational behavior of *N*phe,

*N*spe and *N*rpe was further investigated as a function of chain length by keeping the amide bond geometry both as cis and trans. The conformational states for the various polypeptoids were generated from the knowledge of Φ, Ψ, ω values corresponding to model dipeptoids given in Table 1 and their energy computed. The results obtained are summarized in Table 2 and 3.

As expected *N*phe peptoids adopted degenerate conformations of opposite handedness with Φ, Ψ values of approximately ± 120°, ± 150° with trans amide bond geometry (Table 2). These states are characterized by θ = ± 111°, number of residues per turn i.e. n = 3.24 and rise per residue; h ~ ± 3.25 Å. Stability of these states arises due to: i) carbonyl…carbonyl interactions between adjacent carbonyl groups of peptoid backbone ($do_i…c_{i+1}$ being in the range 3.5 to 3.8 Å), ii) stacking interactions between carbonyl groups and aromatic rings; the distance of carbonyl group from one edge of aromatic ring being in the range 2.0 to 4.0 Å [64-66] and iii) edge to edge stacking interactions between the aromatic side chains. Further, carbonyl…carbonyl interactions were found to be of the sheared parallel motif and importance of these interactions as a stabilizing factor in α-helices, β-sheets and right handed twist and peptoids is well documented [67-75].

Degeneracy between these states was lifted with an increase in chain length. This observation was better realized with trans amide bond geometry and the right handed structure with Φ, Ψ values of -120°, -150° was favored due to built up of stronger carbonyl…carbonyl interactions as the oligomer chain length grew. Such structures may be realized in aprotic solvents of low polarity that are not capable of interacting with the backbone. These findings are well supported by X-ray crystallographic studies on achiral *N*-hydroxy amide containing peptoids with no chirality in side chain [35] and QM calculations on similar *N*-aryl peptoid oligomers [32]. It is worth mentioning here that peptoids containing *N*-hydroxy amides have been synthesized using DMF as a solvent at the coupling stage and the crystals grown from aprotic $CHCl_3$/n-hexane solvent.

Introduction of chirality in peptoid side chain creates an asymmeterical environment around the backbone. Therefore, conformational studies on *N*spe/*N*rpe peptoids having chirality in their side chains were carried out as a function of chain length both in the presence and absence of protecting groups, and keeping the amide bond geometry cis as well as trans. The results for model tri and hexapeptoids are summarized in Table 3. Model dipeptoids Ac-*N*spe/*N*rpe-NMe_2 were found to be degenerate on the energy scale with Φ, Ψ values of 120°, 150° & -110°, -165° respectively with trans amide bond geometry and states with cis amide bond geometry were ~ 4 kcal mol^{-1} higher in energy (Table 1). This degeneracy was lifted in favor of *N*spe polypeptoids with an increase in chain length and Ac-*N*spe_5-NMe_2 and Ac-*N*rpe_5-NMe_2 were found to be populated in the conformational states with Φ, Ψ values of ~ 110°, 160° and -110°, -160° respectively. It is rather surprising and interesting that *N*spe oligomers favored left handed structure and *N*rpe oligomers favored right handed structure. Molecular view of Ac-*N*spe_5-NMe_2 and Ac-*N*rpe_5-NMe_2 in the most stable states depicting the various interactions (Figure 2) clearly reveals that the π…π interactions between aromatic rings are favored in Ac-*N*spe_5-NMe_2 and hence, accounts for the espousal of the left handed structure.

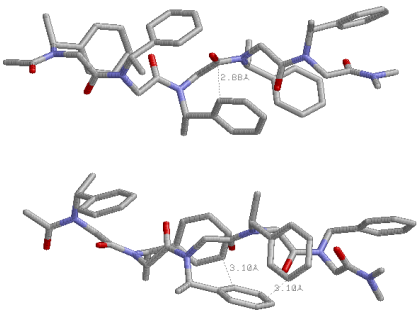

Figure 2. Molecular view in the most stable conformation of Ac-*N*spe_5-NMe_2 with Φ, ψ, ω values ~ 100°, 150°, 180°, and Ac-*N*rpe_5-NMe_2 with Φ, ψ, ω values ~ -100°, -150°, 180° showing stacking interactions between carbonyl moieties and aromatic rings and π…π interactions between aromatic rings.

Role of Protecting Groups: To gain further insight on the role of interactions stabilizing the peptoid Ac-*N*spe_5-NMe_2 over Ac-*N*rpe_5-NMe_2, conformations of these peptoids without protecting groups i.e. -(*N*spe/*N*rpe)$_{2/6}$-NH_2 were studied and the results summarized in Table 3. A large change in the χ value of the first peptoid residue with a little or no change in χ values of the other residues was observed as compared to the χ values of the peptoid residues in corresponding models with protecting group. Interestingly, -*N*$rpe_{2/6}$-NH_2 was predicted to be more stable than the peptoid -*N*$spe_{2/6}$-NH_2 and adopted polyproline type II structure like the corresponding model peptoid with protecting groups. This has been attributed to the one pair of carbonyl…carbonyl interactions being less due to the absence of the acetyl group.

It is obvious from the molecular view of (*N*rpe/*N*rpe)$_{2/6}$-NH_2 shown in Figure 3 that the stacking interactions between carbonyl groups and one edge of the aromatic rings of the same residue are stronger in -*N*$rpe_{2/6}$-NH_2 as compared to -*N*$spe_{2/6}$-NH_2 and this type of stacking interactions is well accepted [64-66]. In -*N*$spe_{2/6}$-NH_2 three conformational states; one with trans amide bonds and two with cis amide bonds with Φ, ψ values inverse of each other (i.e. opposite handed) were found to be degenerate (Table 3). Thus, it is quite likely that in solvents with very low dielectric constant not capable of interacting with backbone, -*N*$spe_{2/6}$-NH_2 may exhibit a very weak signal in CD spectroscopy.

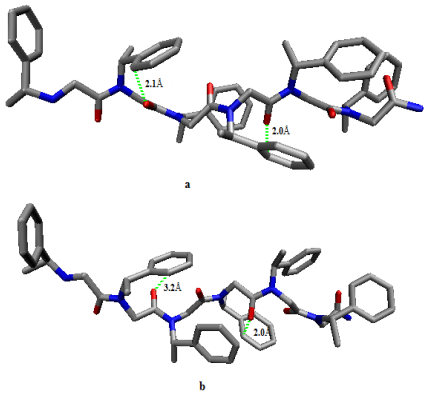

Figure 3. Molecular view of the peptoids (a) -*N*rpe_6-NH_2 and (b) -*N*spe_6-NH_2 depicting stronger carbonyl and aromatic interactions in -*N*rpe_6-NH_2.

Table 2: Conformational results* for the peptoids the Ac-*N*phe$_n$-NMe$_2$, as a function of chain length (n = 2-7) with trans and cis amide bond geometries

i) trans amide bonds

Residue Number							
1	2	3	4	5	6	7	ΔE (kcal/mol)
-120, -150	**-120, -150**						
176	*172*						0
135, 110	140, 110						
115, 160	**120, 150**						
-176	*-172*						0.7
-135, -110	-140, -110						
105, 160	**115, 160**	**120, 155**					
-178	*-166*	*180*					0
-160, -105	-155, -105	-145, -105					
-105, -160	**-115, -160**	**-120, -150**					
178	*170*	*180*					0.3
160, 100	155, 105	140, 110					
-105, -160	**-115, -165**	**-120, -155**	**-120, -145**				
178	*168*	*180*	*164*				0.0
160, 100	160, 100	140, 110	145, 110				
115, 170	**110, 170**	**120, 165**	**115, 165**				
180	*170*	*-178*	*174*				1.0
-145, -100	-140, -105	-160, -95	-145, -105				
-110, -160	**-115, -175**	**-110, -175**	**-110, -175**	**-120, -150**			
176	*168*	*178*	*172*	*180*			0.0
165, 100	160, 100	160, 100	155, 100	140, 110			
120, 155	**115, 160**	**120, 155**	**115, 160**	**120, 155**			
-176	*-174*	*-170*	*-176*	*-172*			5.5
-135, -110	-165, -100	-135, -110	-165, -100	-145, -105			
-110, -160	**-115, -160**	**-115, -165**	**-115, -160**	**-115, -155**	**-120, -150**		
178	*174*	*-176*	*172*	*174*	*168*		0.0
155, 105	155, 105	160, 100	135, 110	135, 115	140, 110		
110, 165	**110, 165**	**115, 155**	**115, 155**	**120, 155**	**120, 150**		
-178	*-174*	*178*	*-166*	*-166*	*-168*		6.7
-160, -100	-140, -110	-135, -115	-135, -110	-135, -110	-140, -110		
-105, -165	**-105, -165**	**-105, -165**	**-105, -165**	**-105, -160**	**-115, -160**	**-120, -160**	
180	*174*	*176*	*176*	*178*	*180*	*180*	0
155, 105	155, 105	150, 105	150, 105	155, 105	160, 100	150, 100	
115, 160	**110, 160**	**115, 160**	**110, 160**	**115, 160**	**110, 160**	**110, 165**	
175	*180*	*176*	*176*	*-178*	*176*	*168*	9.1
-135, -110	-150, -105	-145, -110	-150, -105	-140, -110	-145, -110	-145, -105	

ii) cis amide bonds

ii) cis amide bonds-	**-120, -150**						
115, -160							
0	*4*						1.5
140, 110	140, 110						
115, 160	**120, 150**						
0	*0*						1.6
-140, -110	-145, -105						
-115, -160	**-115, -160**	**-120, -150**					
0	*-8*	*-6*					8.2
140, 110	140, 110	140, 110					
115, 160	**115, 160**	**120, 150**					
-2	*0*	*6*					9.4
-140, -110	-140, -110	-140, -110					
-115, -160	**-115, -160**	**-120, -155**	**-125, -150**				
0	*-6*	*-6*	*-12*				9.5
140, 110	140, 110	150, 105	150, 100				
115, 160	**115, 165**	**120, 155**	**120, 155**				
0	*0*	*6*	*6*				10.6
-140, -110	-145, -105	-150, -105	-150, -105				
-115, -160	**-115, -155**	**-120, -155**	**-120, -155**	**-120, -150**			
0	*-8*	*0*	*-2*	*-4*			16.6
140, 110	145, 105	145, 105	145, 105	140, 110			
115, 160	**115, 160**	**115, 160**	**115, 160**	**120, 150**			
0	*2*	*8*	*-4*	*8*			18.3
-140, -110	-140, -110	-140, -110	-140, -110	-140, -110			
115, 160	**115, 160**	**120, 155**	**115, 160**	**120, 155**	**120, 150**		
-2	*4*	*4*	*0*	*10*	*2*		17.4

-140, -110	-145, -105	-145, -105	-145, -105	-145, -105	-140, -110		
-120, -155	**-120, -155**	**-115, -160**	**-120, -155**	**-115, -160**	**-120, -155**		
0	*2*	*-4*	*-4*	*2*	*-6*		18.4
145, 105	145, 105	145, 105	145, 105	145, 105	145, 105		
-120, -150	**-120, -155**	**-120, -150**	**-120, -160**	**-120, -160**	**-120, -155**	**-120, -160**	
2	*0*	*-4*	*-2*	*-6*	*-2*	*-2*	26.8
150, 105	150, 100	150, 105	150, 100	150, 100	150, 105	150, 100	
115, 160	**115, 160**	**120, 150**	**115, 160**	**115, 160**	**115, 160**	**120, 170**	
-2	*0*	*0*	*0*	*4*	*6*	*4*	36.0
-140, -110	-140, -110	-140, -110	-140, -105	-140, -110	-135, -110	-90, -100	

***Φ, Ψ** values are given in **bold text;** *ω* values are *italicized* and χ values are given in normal text

Table 3. Conformational results*(QM) for homo-polypeptoid models

Φ, Ψ, *ω* χi, χj	**Φ, Ψ**, *ω* χi, χj	ΔE kcal/mol	**Φ, Ψ**, *ω* χi, χj	**Φ, Ψ**, *ω* χi, χj	ΔE kcal/mol
	Ac-*N*spe$_2$-NMe$_2$		**Ac-*N*rpe$_2$-NMe$_2$**		
110, 160, *-176*	**110, 160, *-174***	**0.5**	**-110, -160, *180***	**-110, -165, *178***	**0.0**
95, -110	105, -115		-95, 110	-105, 115	
85, -175, *-8*	**80, 180**, *-8*	6.7	**-80, 170,** *6*	**-80, -175**, *4*	6.6
-125, 125	-120, 120		130, -130	120, -120	
-65, 165, *-8*	**-75, 180, *0***	**7.3**	**65, -165, *8***	**70, -160, *4***	**7.4**
-120, 125	-130, 130		120, -120	125, -125	
	-*N*spe$_2$-NH$_2$		**-*N*rpe$_2$-NH$_2$**		
-, 100, *176*	**110, -175, *-178***	**2.6**	**-, 110, *165***	**-110, -165, *178***	**0.0**
115, 130	120, 110		-175, 65	-110, 115	
-, 120, *5*	**-90, 175, *-4***	**2.6**	**-, 110, *-18***	**80, -160, *-2***	**1.9**
150, 0	-130, 125		-175, 65	-150, 5	
-, 95, *-8*	**70, -155, *4***	**3.1**	**-, 110, *8***	**-100, 170, *-2***	**2.4**
85, 130	-125, 130		-175, 65	-125, -115	

Residue Number						ΔE kcal/mol
1	**2**	**3**	**4**	**5**	**6**	
			Ac-*N*spe$_5$-NMe$_2$			
110, 165, *-179*	**110, 160, *-175***	**95, 150, *-177***	**110, 160, *180***	**120, 150, *-177***		**0**
85, -155	115, -125	110, -120	105, -115	105, -115		
			Ac-*N*rpe$_5$-NMe$_2$			
-110, -165, *177*	**-105, -160, *-177***	**-105, -160, *-174***	**-105, -165, *-176***	**-90, -160, *179***		**2.3**
-90, 105	-100, 115	-100, 115	-115, 120	-85, 115		
-*N*rpe$_6$-NH$_2$						
-, 180, *178*	**-105, -170, *-176***	**-105, -175, 178**	**-105, -175, *-176***	**-105, -165, *178***	**-115, -155, *176***	**0**
150, -125	-115, 115	-95, 105	-95, 105	-90, 105	-110, 120	
-, -170, *-2*	**80, 175, *6***	**100, -165, *0***	**90, 170, *2***	**70, -170, *2***	**65, -165, *8***	**7.78**
-40, -125	125, -125	125, -125	125, -125	125, -125	125, -125	
-*N*spe$_6$-NH$_2$						
-, 180, *-179*	**110, 160, *176***	**90, 160, *180***	**110, 160, *180***	**90, 160, *180***	**115, 155, *-177***	**8.0**
-155, 130	115, -120	115, -120	115, -120	115, -120	110, -120	
-, 175, *-6*	**-105, -175, *-4***	**-90, 180, *0***	**-85, 175, *-2***	**-85, 165, *-2***	**-95, 165, *-4***	**8.2**
155, -10	-130, 130	-125, 125	-125, 125	-120, 120	-120, 120	
-, 175, *2*	**85, 170, *6***	**90, 180, *-2***	**90, 175, *-5***	**85, -175, *-2***	**75, 175, *-4***	**8.7**
165, -20	-130, 130	-130, 125	-120, 120	-120, 120	-120, 120	

***Φ, Ψ, *ω* values are given in bold text;** and χ values are given in normal text

Table 4. Torsion angles for the peptoid Ac-*N*phe$_7$-NMe$_2$ after simulation (1ns) in water with different starting conformations (I-IV)*

St Conf	Φ	Ψ	*ω*	χi, χj	St Conf	Φ	Ψ	*ω*	χi, χj
I	**43.8**	**-145.3**	***-159.6***	**-120.2, 76.7**	**II**	**-66.8**	**136.8**	***-159.8***	**123.2, -65.7**
	73.1	**-139.9**	***174.9***	**113.9, -44.9**		**-75.8**	**-178.1**	***168.6***	**117.3, 116.2**
	49.7	**-129.5**	***-169.5***	**84.1, -113.3**		**-69.2**	**124.9**	***163.9***	**-83.3, 98.8**
	61.7	**-117.5**	***-167.9***	**-136.4, 75.6**		**-62.2**	**119.9**	***175.7***	**95.0, -74.3**
	79.1	**-142.2**	***-175.0***	**-99.8, 54.7**		**-43.6**	**139.4**	***172.6***	**97.8, 132.8**
	87.8	**173.6**	***-176.2***	**112.8, -69.9**		**-120.4**	**-165.5**	***-177.7***	**98.7, -59.7**
	73.1	**-125.8**	***-178.4***	**-105.7, 79.6**		**-75.7**	**124.5**	***179.7***	**-101.1, 79.4**
III	**84.9**	**176.5**	***7.8***	**-85.0, 93.5**	**IV**	**-101.9**	**-132.6**	***-3.3***	**59.6, -129.6**
	87.5	**159.2**	***-23.3***	**-69.6, 84.3**		**-118.8**	**-108.2**	***-9.7***	**54.1, -110.8**
	116.7	**-169.5**	***-5.9***	**119.8, -87.8**		**-90.5**	**-175.5**	***-3.2***	**-99.7, 75.7**
	101.5	**142.1**	***-12.9***	**-45.3, 109.2**		**-87.0**	**-162.5**	***-3.3***	**94.1, -59.6**

	76.6	**172.6**	***8.9***	**87.7, -122.7**		**-96.6**	**-158.4**	***-16.7***	**89.9, -61.0**
	84.5	**-171.8**	***-19.9***	**-61.6, 82.5**		**-77.9**	**162.0**	***-1.2***	**85.2, -80.5**
	98.3	**129.1**	***-3.8***	**-103.2, 80.6**		**-97.5**	**-144.8**	***11.4***	**86.4, -75.6**

*Starting conformations (St Conf) - I: **Φ, Ψ**, ω ~ 120°, 180°, 180°; II: **Φ, Ψ**, ω ~ -120°, 180°, 180°; III: **Φ, Ψ**, ω ~ 120°, 180°, 0°; IV: **Φ, Ψ**, ω ~ -120°, 180°, 0°

Table 5. Simulation (1ns) results in terms of **Φ, ψ,** ω, χ_i, χ_j **values in degrees for peptoids under NVT conditions in water and DMSO**

In Water

	1	**2**	**3**	**4**	**5**	**6**	ΔE kcal/mol
Ac-*N*spe$_5$-NMe$_2$							
-94.1, -160.1	**-95.6, -154.1**	**-100.1, -135.6**	**-86.0, 166.0**	**-96.5, -120.0**			0
-2.4	*-16.0*	*-7.8*	*-1.8*	*3.0*			
-42.8, -49.2	-74.8, -100.6	-49.1, -39.1	-43.2, -47.5	-58.0, -74.7			
61.9, -130.0	**84.5, -165.6**	**62.7, -130.3**	**62.8, -138.8**	**94.7, 146.3**			2.4
-166.3	*179.3*	*-172.7*	*170.8*	*166.9*			
91.9, -104.1	109.8, -73.5	112.6, -71.8	130.9, -60.9	121.6, -97.4			
-65.1, 156.0	**-65.9, 141.8**	**-68.2, 149.4**	**-75.1, 171.6**	**-70.4, 141.8**			2.6
160.1	*-178.2*	*171.1*	*170.7*	*-168.4*			
113.2, -95.8	143.2, -74.9	109.3, -93.8	103.2, -83.9	133.1, -82.1			
74.2, -145.3	**105.5, 141.0,**	**95.7, 162.4**	**83.2, 171.0**	**76.6, 135.0**			6.3
1.5	*-14.9*	*8.3*	*-0.4*	*16.5*			
104.2, -83.9	135.4, -86.9	101.9, -89.7	115.6, -99.1	-78.9, 105.9			
Ac-*N*rpe$_5$-NMe$_2$							
86.1, 152.6	**77.2, 138.8**	**82.9, 163.7**	**91.2, -158.3**	**96.3, 134.9**			0.2
5.5	*6.1*	*26.1*	*-0.3*	*-12.9*			
49.1, 74.6	64.7, 74.4	34.5, 69.5	-139.8, 54.2	43.9, 29.6			
-75.8, 158.0	**-60.3, 122.8**	**-88.3, 176.8**	**-68.5, 124.0**	**-58.8, 141.3**			2.1
-173.6	*156.3*	*-174.7*	*170.1*	*-178.7*			
-113.9, 85.5	-102.1, 96.8	-110.0, 103.3	-129.7, 77.8	-129.6, 66.9			
63.8, -155.5	**63.1, -129.8**	**74.0, -130.0**	**61.6, -122.5**	**65.6, -118.4**			2.3
-174.6	*-179.5*	*-166.0*	*162.2*	*176.3*			
-135.6, 73.8	-145.1, 33.7	-106.8, 81.7	-122.4, 93.8	-122.1, 74.3			
-78.0, 162.7	**-66.2, 173.4**	**-80.7, -170.9**	**-77.0, -159.4**	**-61.8, 179.**			4.4
-9.5	*-18.0*	*-4.4*	*-18.8*	*, -25.0*			
-98.7, 97.2	-119.4, 96.1	53.0, 43.9	69.2, 86.1	73.8, 89.4			
-*N*spe$_6$-NH$_2$							
-, -172.6	**69.3, -172.6**	**79.4, -120.3**	**83.7, -164.1**	**55.5, -144.8**	**74.9, -144.7**		0
-177.5	*-163.6*	*175.9*	*-171.2*	*147.4*	*-178.8*		
129.8, -68.0	115.4, -79.7	92.8, -95.4	123.6, -83.2	130.5, -73.2	114.8, -88.5		
-, 142.4	**-98.1, -153.1**	**-101.1, -158.4**	**-95.6, -133.9**	**-91.5, -147.5**	**-84.4, 174.4**		7.5
-4.7	*-4.0*	*-2.2*	*9.8*	*3.8*	*9.5*		
160.9, -46.3	-66.7, -67.6	149.4, -54.5	-61.6, -57.7	-56.7, -23.6	-59.9, -83.8		
-, 167.9	**-67.1, 128.3**	**-58.8, 121.1**	**-66.7, 135.9** *174.9*	**-54.6, 160.9**	**-64.9, 179.8**		7.6
-164.6	*-165.2*	*-169.2*		*-178.9*	*-176.2*		
105.2, 126.8	113.1, 132.6	115.9, 116.3	145.0, 131.0	113.5, 75.7	98.2, 88.9		
-, -141.5	**76.2, 146.2**	**78.0, 148.1**	**67.2, -167.9** *6.9*	**83.0, 150.3**	**63.9, 157.0** *12.5*		8.9
1.3	*6.0*	*-0.7*		*31.3*			
141.7, -25.3	107.7, -84.7	103.8, -106.3	114.2, -93.4	-67.2, -33.8	-65.8, -57.8		
-*N*rpe$_6$-NH$_2$							
-, 166.3	**-69.7, 143.1**	**-73.9, -177.7**	**-64.3, 137.9**	**-68.4, 177.2**	**-64.2, 152.1**		1.0
-170.6	*168.1*	*156.2*	*164.5*	*-170.5*	*-167.6*		
-147.2, 43.5	-111.5, 94.3	-107.8, 93.2	-113.9, 88.8	-106.3, 84.2	-131.1, 88.7		
-, -163.8	**100.3, 154.3**	**78.6, -160.1**	**85.8, 164.0**	**102.1, 147.7**	**85.2, 115.4**		3.0
4.5	*9.5*	*-10.3*	*-5.6*	*8.0*	*6.2*		
-172.0, -135.8	51.5, -147.6	47.9, -120.6	60.7, -135.7	55.3, -100.1	43.9, -117.9		
-, 152.8	**63.8, -145.4**	**63.1, -142.2**	**69.3, -137.2** *-174.7*	**80.6, -147.8** *-161.2*	**46.2, -143.1** -		8.0
-168.2	*-160.6*	*169.7*			*171.0*		
-140.7, 59.2	-120.6, 108.8	-116.8, 78.2	-103.7, 91.9	-139.0, 52.1	-117.6, 77.4		
-, -151.3	**-72.2, 143.0**	**-73.3, 155.6** *-10.8*	**-77.2, 162.4** *-31.8*	**-84.2, -153.9** *-10.9*	**-97.6, -149.4**		11.8
-9.1	*17.9*				*21.5*		
-126.3, 45.7	-122.5, 74.9	-119.2, 96.1	63.1, 57.7	67.9, 73.6	52.1, 55.8		

In DMSO

Ac-Nspe$_5$-NMe$_2$						
-83.4, -135.7	**-92.1, -118.4**	**-77.0, 162.9**	**-88.6, -145.8**	**-91.8, -142.0**		1.5
-19.1	*-22.3*	*7.3*	*15.9*	*5.1*		
-39.6, -27.2	-58.0, -77.8	-55.9, -64.3	-41.7, -65.3	-46.1, -67.0		
55.8, -136.5	**83.6, -161.3**	**65.4, -117.6**	**47.4, -104.9**	**62.9, -123.0**		5.4
-176.8	*161.2*	*-171.4*	*171.3*	*175.0*		
117.8, -101.3	125.3, -101.1	116.7, -94.2	108.5, -93.2	120.9, -95.2		

81.6, -162.0	**84.1, 153.2**	**100.8, 145.4**	**68.1, -160.4**	**80.0, 132.8**		9.3
10.6	*10.7*	*-13.6*	*-2.2*	*8.9*		
124.0, -91.5	103.8, -99.4	87.1, -92.0	138.3, -54.5	-60.0, -74.4		
-65.6, 141.5	**-79.4, 164.5**	**-65.1, 106.3**	**-47.5, 124.7**	**-83.8, 91.3**		10.4
-176.5	*163.3*	*-158.6*	*-161.6*	*-172.3*		
111.4, -66.9	146.3, -35.1	112.2, -73.8	100.5, -82.7	113.4, -88.2		
Ac-Nrpe$_5$-NMe$_2$						
-75.6, -167.3	**-70.2, -145.7**	**-77.7, 158.4**	**-88.5, -137.0**	**-107.7, -157.3**		0
-3.3	*-16.3*	*6.5*	*9.0*	*6.9*		
-135.3, -137.3	-131.8, -99.2	66.4, -138.7	67.1, -85.3	45.6, -131.6		
71.9, 170.9	**62.5, -159.7**	**89.7, 131.9**	**70.4, -164.3**	**78.9, 142.6**		1.2
9.5	*22.9*	*6.8*	*-7.4*	*2.4*		
45.3, 42.8	45.2, 28.2	59.9, 97.0	-138.9, 67.4	63.7, 90.8		
-71.8, 139.8	**-67.2, 120.7**	**-74.5, 124.7**	**-63.5, 122.8**	**-69.6, 139.0**		7.4
-171.9	*158.6*	*-172.9*	*-167.7*	*176.9*		
-124.1, 71.1	-103.2, 95.3	-117.2, 89.9	-108.3, 101.8	-123.9, 82.3		
61.2, -136.5	**70.0, -153.1**	**52.4, -151.1**	**77.6, -152.9**	**55.8, -113.1**		8.5
-172.6	*-157.4*	*-157.4*	*-164.2*	*-173.0*		
-142.4, 71.4	-108.3, 88.7	-116.8, 71.8	-129.4, 67.4	-118.8, 70.1		
-Nspe$_6$-NH$_2$						
-, 164.6	**97.9, 141.0**	**71.0, 166.9**	**93.3, 147.6**	**84.6, 156.6**	**72.1, 161.2**	0
-2.6	*15.3*	*17.7*	*3.7*	*26.4*	*4.3*	
99.5, -69.4	111.7, -81.5	150.3, -60.6	-75.0, -86.3	-56.5, -72.2	-72.0, 155.2	
-, 130.6	**-82.3, 172.6**	**-72.7, -161.7**	**-104.1, -125.0**	**-99.0, -159.4**	**-78.7, -144.4**	1.4
-9.5	*-15.7*	*-2.0*	*-5.1*	*-16.6*	*-4.4*	
-125.6, 125.6	113.8, 108.5	-64.1, 67.0	-59.7, 95.9	-62.1, 97.2	-82.1, 66.2	
-, -166.3	**63.7, -123.9**	**69.0, -124.2**	**77.3, -131.7**	**65.9, -136.6**	**60.8, -146.6**	7.3
174.9	*-176.1*	*-178.0*	*-170.0*	*-174.2*	*-172.8*	
151.6, -52.9	106.7, -74.8	120.5, -77.7	114.0, -91.5	121.8, -68.2	133.3, -51.7	
-, 170	**-71.9, 142.1**	**-69.1, 143.5**	**-53.0, 110.9**	**-44.6, 112.4**	**-68.8, 142.2**	8.6
-176.1	*-177.8*	*-175.7*	*-163.7*	*-165.9*	*168.6*	
165.5, -57.6	112.4, -82.7	117.8, -83.6	108.2, -83.2	105.1, -78.4	127.8, -70.2	
-Nrpe$_6$-NH$_2$						
-, -153.1	**71.5, -175.9**	**82.6, 162.5**	**81.6, 157.4**	**86.5, 155.9**	**107.9, 140.3**	1.1
14.5	*10.0*	*0.9*	*12.8*	*-32.6*	*5.0*	
110.5, 137.5	113.8, 107.6	108.9, 107.4	-62.4, 89.1	-60.6, 132.2	-55.0, 132.4	
-, -161.2	**54.8, -113.2**	**65.6, -140.9**	**75.4, -146.7**	**77.8, -111.3**	**81.4, 140.8**	4.4
179.1	*179.2*	*-171.9*	*-154.9*	*178.3*	*-176.1*	
114.1, -33.1	144.7, -20.1	128.6, -102.9	89.6, -83.8	83.9, -98.1	110.4, -94.2	
-, -151.3	**-79.6, 169.9**	**-71.7, 178.0**	**-55.9, 161.0**	**-84.4, -140.2**	**-77.5, -159.5**	4.6
-6.8	*3.5*	*-15.0*	*-2.5*	*-10.4*	*-10.4*	
-161.3, -118.5	-101.2, -91.5	-118.2, -91.4	50.8, -112.8	55.1, -113.0	57.5, -99.7	
-, 172.9	**-71.9, 120.9**	**-72.7, 133.7**	**-67.9, 126.6**	**-72.0, 118.7**	**-86.5, -150.2**	4.8
-170.0	*-160.7*	*-176.6*	*-173.3*	*169.6*	*169.6*	
-112.4, -126.8	-129.7, -67.5	-157.7, -133.6	-116.5, -108.6	-111.9, -66.6	-110.6, -88.8	

3.2 MD Simulation Studies

The starting geometries for simulation studies in water & DMSO were taken from quantum mechanical calculations and correspond to states with Φ, Ψ and ω values of ~ 90°, 150°, 180°; -90°, 180°, 180°; 0°, 90°, 180°; 0°, -90°, 180°; 90°, 150°, 0°; -90°, 160°; 0°, 0°, 90°, 0°; and 0°, -90°, 0° (the 0°, ± 90° states were predicted only with trans amide bond geometry). Simulation results revealed population of a state with Φ, Ψ values of ~ 60°, -150° when the starting geometries had Φ, Ψ & ω values of 90°, 150°, 180° or 0°, -90°, 180° and with starting conformational states having Φ, Ψ, ω values of -90°, 180°, 180° or 0°, 90°, 180° the peptoids were found to adopt polyproline type II like structure. Therefore, only the results corresponding to four different starting conformations are discussed and summarized.

Simulations in Water: As Φ, Ψ values of ~ 60°, -150° are inverse of the Φ, Ψ values in poly-L-proline (PP) with ω = 180°, this conformational state has been referred as *inverse*-poly-L-proline type-II. Likewise, the state with repeated Φ, Ψ and ω values of ~ 60°, -150°, 0° has been named inverse PP-I helix. In all peptoids with starting geometry having Φ, Ψ and ω values of 90°, 150°, 180° the inverse PP-II structure was populated whereas with Φ, Ψ and ω value of -90°, 180°, 180° as starting conformation the PP-II structure was obtained. PP-I and inverse PP-I structures were realized with starting geometries having Φ, Ψ and ω values of ~ -90°, 180°, 0° and 90°, 180°, 0° respectively.

It is apparent from the results in Table 4 that Ac-*N*phe$_7$-NMe$_2$ adopts helices of opposite handedness i.e. PP-II and inverse PP-II and PP-I and inverse PP-I. The driving force for population of these states came from hydrogen bond interactions between water molecules and the carbonyl oxygens. It is rational to think that the no signal in CD spectroscopic studies may be explained in terms of population of such opposite handed structures of the same types and to the same extent. Thus, these computational results provide an excellent explanation to the no net CD signal [28] reported for such peptoids. Similar results have also been reported for oligo (*N*-aryl glycine) where the aromatic ring is directly attached to the backbone N-atom [32].

Simulations under NVT Conditions: In order to have a quantitative explanation on the energy scale, simulations of Ac-*N*spe$_5$/*N*rpe$_5$-NMe$_2$ with different starting conformations were performed under NVT conditions. The results summarized in Table 5 reflect interesting observations on these peptoids as they are found to be equally stable (on the energy scale) with cis amide bond geometry; adopting conformations of opposite handedness with average Φ, Ψ values of ~ -90°, -155° (PP-I type) and 90°, 155° (inverse PP-I type). In other words, chirality of the sidechain dictates

handedness of the adopted structures and χ values of the sidechain correspond to anti gauche and gauche region respectively. Quantum mechanical calculations predict these states to be higher in energy (Table 1, 2 and 3) and thus the role of solvent water molecules in stabilizing these structures is obvious. The polyproline type II conformation with average Φ, Ψ values of -70°, 150° and inverse-polyproline type II conformation with Φ, Ψ values of 70°, -135° were also degenerate in both these molecules but lied ~ 2.2 kcal mol^{-1} higher in energy. Similar results have been reported on *N*-aryl peptoid oligomer by *ab initio* calculations [32]. Analysis of the results as a function of time in blocked as well as unblocked polypeptoids with different starting geometries revealed that no inter-conversion of the amide bond geometry takes place i.e. cis remains in cis and trans remains in trans geometry and the deviations in ω values of ~ ± 20° is caused by interaction of water molecules with carbonyl groups of backbone. Further, the π…π interactions between aromatic rings as observed in QM results also disappears. Also, interactions between solvent water molecules and carbonyl oxygens of peptoid backbone were more favorable with cis amide bonds than with trans amide bond geometry. Water molecules were involved in hydrogen bond formation with the carbonyl moieties of amide linkages and the distance between the carbonyl oxygen of the peptoid backbone and hydrogen of water was 1.75 ± 0.15 Å with $d_{O\cdots O}$ being 2.7 ± 0.20 Å and the angle ∠OHO lying between 155° to 175°. This observation is consistent with the experimental fact that in biological systems the hydrogen bond is rarely linear [76]. However, the CD spectrum characteristics of homo-*N*spe and *N*rpe peptoids are reported to be similar to that of right handed and left handed helices in peptides respectively [29,32]. The observed CD spectroscopic results for peptoids can be explained in terms of the interactions between the backbone and aromatic ring chromospheres like in Gramicidin A [77,78]. A molecular view of these molecules with water molecules within 3 Å of the peptoid surface shown in Figure 4 clearly reveals the interaction between i) carbonyl oxygen of the backbone and water molecules, ii) carbonyl groups and $C_{\gamma\text{-}\beta\text{-}\gamma'}$ face of the aromatic ring of the same residue and iii) backbone carbonyl-carbonyl interactions.

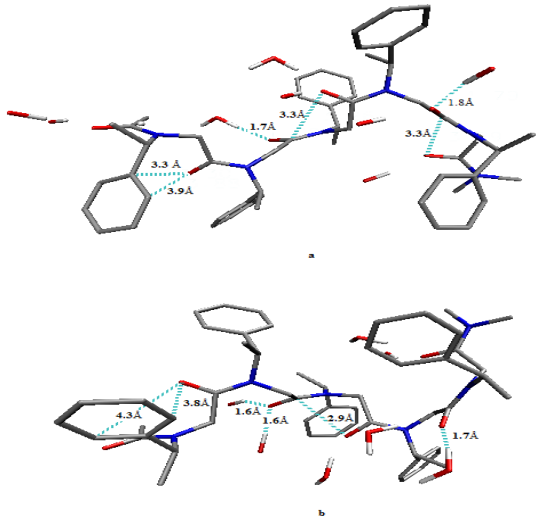

Figure 4. Graphical view of Ac-*N*spe$_5$-NMe$_2$ & Ac-*N*rpe$_5$-NMe$_2$ on simulation in water; depicting carbonyl-carbonyl, carbonyl-aromatic & carbonyl-water interactions and water molecules within 3 Å of the peptoid surface.

Without protecting groups the peptoid -*N*rpe$_6$/*N*spe$_6$-NH_2 populated poly-L-proline and inverse-poly-L-proline type-II helices respectively and -*N*spe$_6$-NH_2 was predicted to be slightly more stable (1 kcal mol^{-1}) as compared to -*N*rpe$_6$-NH_2. Thus, as in peptoids with protecting group the chirality of the side chain dictates the handedness of the adopted structure. PP-II and inverse PP-II structures are highly extended while PP-I and inverse PP-I are found to be more compact. The characteristics of these structures are consistent with the experimental facts and such structures should be almost insensitive to variations in temperature and pH. Conformational stability and rigidity of peptoids adopting PP-II helices can be exploited as molecular spacers like polyproline [79,80] and other biological purposes [81] .

Simulations in Dimethyl sulphoxide: Simulation results in water appear to be somewhat at variance with the experimental results when DMSO [82] is used as a solvent at the coupling stage during peptoid synthesis but the results were found to be in conformity with the results where DMF has been used as a solvent at the coupling stage between a haloacetic acid and the primary amine of interest. Population of PP-I, inverse PP-I, PP-II and inverse PP-II structures in water is mainly attributed to the formation of hydrogen bonds between peptoid backbone carbonyl oxygens and solvent water molecules. Both DMF and DMSO are aprotic solvents only capable of accepting hydrogens. The charges [83,84] on various atoms of both DMF and DMSO molecules are shown in Figure 5. The magnitude of charge on sulfur and oxygen atoms in DMSO is ~ 2.5 times more as compared to carbon and oxygen atoms in DMF. Therefore, to gain better insight, simulation studies were carried out using DMSO as the solvent.

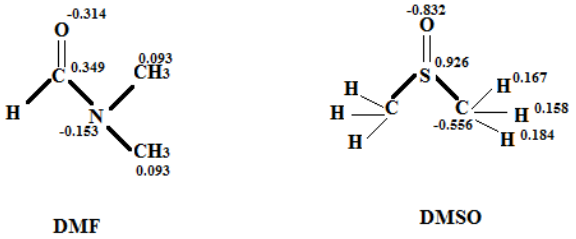

Figure 5: Charges on the various atoms in DMF andDMSO.

Simulation results for Ac-*N*spe$_5$/*N*rpe$_5$-NMe_2 and -*N*spe$_6$/*N*rpe$_6$-NH_2 with different starting conformations are summarized in **Table 5**. It is obvious from the results that both blocked and unblocked peptoid models of *N*spe and *N*rpe were populated in conformations with cis amide bonds and there was hardly any influence of protecting groups. Ac-*N*spe$_5$-NMe_2 adopted a similar conformation as in water and could be realized in PP type-I helix and the inverse PP type-II helix was less stable by 4 kcal mol^{-1}. On the other hand, PP-I and inverse PP-I structures in Ac-*N*rpe$_5$-NMe_2 with Φ, Ψ values of -84°, -162° and 95°, 168° respectively lied within 1.2 kcal mol^{-1} of each other. A molecular view of Ac-*N*rpe$_5$-NMe_2 in both these states is shown in Figure 6. It is apparent from the figure that in DMSO these states were stabilized by interactions of oxygen atoms of DMSO with the carbonyl carbon of the peptoid backbone and electrostatic interactions between the carbonyl oxygen and sulphur moiety of DMSO (these interactions are expected to be much weaker in DMF on the basis of charges). Further, these interactions were found to be weaker in the state with Φ, Ψ values of 95º, 168º (i.e. inverse PP-I structure). Likewise, without protecting

groups -*N*spe$_6$-NH$_2$ was predicted to populate degenerate states with average Φ, Ψ values of 84º, 156º (inverse PP type-I) and -87º, -170º (PP type-I) whereas the peptoid -*N*rpe$_6$-NH$_2$ could be realized only in the left handed helical structure with average Φ, Ψ values of 80.5º, 161º (inverse PP-I). It is rational to argue and propose that it is the direct interaction of DMSO molecules with carbonyl carbons of peptoid backbone that shall lead to the synthesis of peptoids with cis amide bond geometries when DMSO is used as a solvent at the coupling stage between a haloacetic acid and the primary amine; a fact consistent with the experimental observations. Model building also favors the interaction of DMSO with peptoids in cis amide bond geometry over those with trans amide bond geometry. No isomerization of amide bonds was observed but substantial variation in ω values was seen due to interactions with DMSO molecules. Thus, the population of PP type-I and II structures depends on the solvent used and the presence or absence of protecting groups.

4. CONCLUSION

N-substituted glycine monomer units (peptoids) are an important class of sequence specific peptidomimetics known to exhibit diverse biological activities. Conformational preferences of *N*phe, *N*spe and *N*rpe polypeptoids of varying chain length were studied by both quantum mechanical and molecular dynamics approaches. The amide bond geometry was found to be degenerate with ω = 0 ± 20° and 180 ± 20° in model dipepoids. In peptoids of the type Ac-(*N*phe)$_7$-NMe$_2$ having no chiral center in the side chain the degeneracy of the states with Φ, Ψ values of ±120°, ±150° with trans amide bond geometry was lifted with an increase in chain length in favor of the state with Φ, Ψ values ~ -120°, -150° and ω= 180°. *N*spe and *N*rpe peptoids were found to be degenerate on the energy scale with Φ, Ψ values of ~ 110°, 160° & -110°, -160° respectively and *N*spe peptoids were more stable than *N*rpe peptoids with increasing chain length. Stability of these states has been explained in terms of various non-covalent interactions like carbonyl-carbonyl, carbonyl-aromatic and stacking interactions. Such states may be realized in aprotic solvents with low dielectric constants.

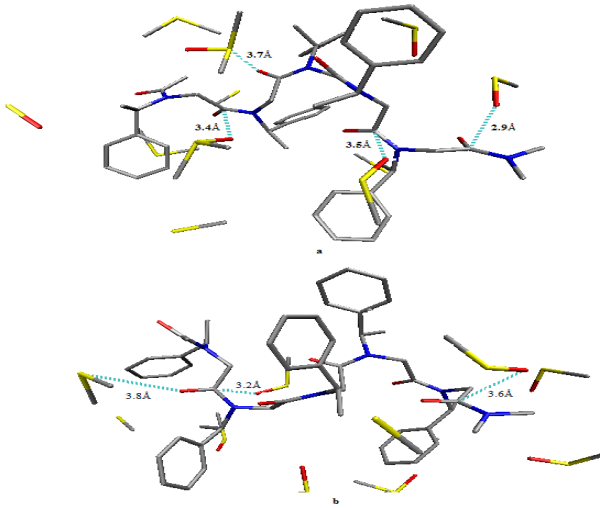

Figure 6. A molecular view of the peptoid Ac-*N*rpe$_5$-NMe$_2$ in conformational states with average Φ, Ψ values of -84°, -162° & 95°, 168° after 1ns simulation in DMSO showing interactions between sulphoxide moiety of DMSO and carbonyl group of peptoid backbone.

Simulation studies in water and DMSO unraveled that no inter-conversion of the amide bond takes place during simulations and the peptoids with protecting groups were predicted to be most stable with cis amide bond geometries in both solvents. This has been explained in terms of interactions of solvent water molecules with carbonyl oxygen of backbone and that of DMSO through its oxygen atom with the carbonyl carbon of peptoid backbone. DMSO was also found to interact electrostatically with the carbonyl oxygen through its sulphur atom. Simulation studies also through light on the role of solvent during peptoid synthesis. Ac-*N*spe$_5$-NMe$_2$ adopted polyproline type I structure in both water and DMSO whereas Ac-*N*rpe$_5$-NMe$_2$ was found to adopt inverse poly-L-proline type I structure in water and polyproline type I helix in DMSO. Interestingly, in the absence of protecting groups -*N*rpe$_6$-NH$_2$ and -*N*spe$_6$-NH$_2$ populated poly-L-proline type II and inverse poly-L-proline type II helices respectively in water. In DMSO -*N*rpe$_6$-NH$_2$ could be realized in inverse polyproline type I helix and -*N*spe$_6$-NH$_2$ in both inverse and polyproline type I structures.

5. REFERENCES

[1] Miller S M, Simon R J, Ng S, Zuckermann R N, Kerr J M & Moos W H (1995) *Drug. Dev. Res*. 35, 20-32

[2] Kwon Y & Kodadek T (2007) *J. Am. Chem. Soc*. 129, 1508-1509

[3] Miller S M, Simon R J, Ng S, Zuckermann R N, Kerr J M & Moos W H (1994) *Bioorg. Med. Chem. Lett.* 4, 2657–2662

[4] Proulx C, Yoo S, Connolly M D & Zuckermann R N (2015) *J. Org. Chem.*, Article ASAP

[5] Huang M L, Benson M A, Shin S B Y, Torres V J & Kirshenbaum K (2013) *Eur. J. Org. Chem*. 2013, 3560–3566

[6] Huang W, Seo J, Willingham S B, Czyzewski, A M, Gonzalgo M L, Weissman I L & Barron A E (2014) *PLOSOne* 9, e90397

[7] Mojsoska B, Zuckermann R N & Jenssena H (2015) *Antimicrob. Agents Chemother*. 59, 4112-20

[8] Patch J A & Barron A E (2003) *J. Am. Chem. Soc*. 123, 12092-12093

[9] Seurynck S L, Patch J A & Barron A E (2005) *Chem. Biol*. 12, 77-88

[10] Rossa T M, Zuckermann R N, William C R & Frey H (2008) *Neuroscience Letters* 439, 30–33

[11] Statz A R, Meagher R J, Barron A E & Messersmith P B (2005*) J. Am. Chem. Soc.*127, 7972-7973

[12] Statz A R, Meagher R J, Barron A E & Messersmith P B (2008) *Soft Matter* 4, 131–139

[13] Lau K H A, Ren C, Sileika T S, Park S H, Szleifer I & Messersmith P B (2012) *Langmuir* 28, 16099−16107

[14] Ham H O, Park S H, Kurutz J W, Szleifer I G & Messersmith P B (2013) *J. Am. Chem. Soc*. 135, 13015–13022

[15] Wender P A, Mitchell D J, Pattabiraman K, Pelkey E T, Steinman L & Rothbard J B (2000) *Proc. Natl. Acad. Sci. USA.* 97, 13003–13008

[16] Schröder T, Schmitz K, Niemeier N, Balaban T S, Krug H F, Schepers U & Bräse S (2007) *Bioconjugate Chem.* 18, 342–354

[17] Nnanabu E & Burgess K (2006) *Org. Lett*. 8,1259-1262

[18] Shin S B Y, Yoo B, Todaro L J & Kirshenbaum K (2007) *J. Am. Chem. Soc.*129, 3218-3225

[19] Pokorski J K, Jenkins L M M, Feng H, Durell S R, Bai Y & Appella D H (2007) *Org. Lett.* 9, 2381-2383

[20] Nandel F S & Jaswal R R (2013) *Ind J. Biochem. Biophys*. 51, 7-18

[21] Maigret B, Perahia D & Pullman B (1970*) J. Theor. Biol*. 29, 275-291

[22] Subramanian E & Parthasarathy R (1989) *Int. J. Pept. Prot. Res.* 33, 345-347

[23] Armand P, Kirshenbaum K, Falicov A, Dunbarck Jr R L, Dill K A, Zuckermann R N & Cohen F E (1997) *Folding and Design* 2, 369-375

[24] Baldauf C, Günther R & Hofmann H J (2006) *Phys. Biol*. 3, S1–S9

[25] Zuckermann R N, Kerr J M, Kent S B H & Moost W H (1992) *J. Am. Chem. Soc.* 114, 10646-10647

[26] Sui Q, Borchardt D & Rabenstein D L (2007*) J. Am. Chem. Soc.* 129, 12042-12048

[27] Wu C W, Kirshenbaum K, Sanborn T J, Huang K, Zuckermann R N, Barron A E, Patch J A, Dill K A (2003) *J. Am. Chem. Soc.* 125, 13525-13530

[28] Wu C W, Sanborn T J, Huang K, Zuckermann R N & Barron A E (2001) *J. Am. Chem. Soc.* 123, 6778-6784

[29] Wu C W, Sanborn T J, Zuckermann R N & Barron A E (2001) *J. Am. Chem. Soc.* 123, 2958-2963

[30] Kirshenbaum K, Zuckermann R N, Dill K A, Barron A E, Armand P, Goldsmith R & Cohen E (1998). *Proc. Natl. Acad. Sci*. 95, 4303-4308

[31] Jordan P A, Paul B, Butterfoss G L, Renfrew P D, Bonneau R & Kirshenbaum K (2011) *Biopoymers (Peptide Science*) 96, 617-625

[32] Shah N H, Butterfoss G L, Nguyen K, Yoo B, Bonneau R, Rabenstein D L & Kirshenbaum K (2008) *J. Am. Chem. Soc*. 130, 16622-16632

[33] Zhang S, Prabpai S, Kongsaeree P & Arvidsson P I (2006) *Chem. Commun* 497-499

[34] Fowler S A, Luechapanichkul R & Blackwell H E (2009) *J. Org. Chem*. 74, 1440–1449

[35] Stringer J R, Crapster J A, Guzei I A & Blackwell H E (2011*) Biopolymer peptide Science* 96, 604-616

[36] Stringer J R, Crapster J A, Guzei I A & Blackwell H E (2010) *J. Org. Chem.* 75, 6068-6078

[37] Stringer J R, Crapster J A, Guzei I A & Blackwell H E (2011) *J. Am. Chem. Soc.* 133, 15559-15567

[38] Qiu Y, Chen P, Guo P, Li Y & Liu M (2008) *Advanced Materials* 20, 2908-2913

[39] Moretto A, Peggion C, Formaggio F, Crisma M, Kaptein B, Boxteman Q B & Toniolo C (2005) *Chirality* 17, 481-487

[40] Pullman B & Pullman A (1974) *Adv. Protein Chem*. 28, 347-526

[41] Lawrence R P & Thompson C(1982) *J. Mol. Str: Theochem*. 88, 37-43

[42] Aleman C & Casanovas J (1994) *Chem Soc Perkins Trans* 2, 563-568

[43] Aleman C & Casanovas J (1995) *Biopolymers* 36, 71-82

[44] Nandel F S & Khare B (2005) *Biopolymers* 77, 63-73

[45] Nandel F S, Malik N, Singh B & Jain D V S (1999) *Int. J. Quant. Chem*. 72, 15-23

[46] Nandel F S, Malik N, Singh B & Virdi M (1999) *Indian J. Biochem. Biophys*. 36, 195-203

[47] Weiner S J, Singh U C, Donell T J O & Kollman P A (1984) *J. Am. Chem. Soc.* 106, 6243-6245

[48] Mohle K & Hoffman H J (1998) *J. Pept. Res*. 51, 19-28

[49] Aduzbei A A & Sternberg J E (1993) *J. Mol. Biol*. 229, 472-493

[50] Adzubei A A, Eisenmenger F, Tumanyan V G, Zinke M & Esipova NG (1987) *Biophys Biochem Res Commun* 146, 934-938

[51] Van der Spoel D, Lindahl E, Hess B, Groenhof G, Mark A E & Berendsen H J C (2005*) J. Comp. Chem*. 26, 1701–1718

[52] Butterfoss G L, Renfren P D, Kuhlman B & Kirshenbaum K A (2009) *J. Am. Chem. Soc*. 131, 16798-16807

[53] Schuettelkopf A W & Van Aalten D M F (2004) *Acta Crystallogr*. D60, 1355-1363

[54] Berendsen H J C, Postma, J P M, Van Gunsteren W F & Hermans J (1981) *In B. Pullman, editor, Intermolecular Forces, Dordrecht: D. Reidel Publishing Company*,331–342

[55] Liu H, Muller-Plathe F & Van Gunsteren W F (1995) *J. Am. Chem. Soc*. 117, 4363-4366

[56] Van Gunsteren W F, Billeter S R, Eising A A, Hünenberger P H, Krüger P, Mark A E, Scott W R P & Tironi I G (1996) Biomolecular Simulation: The GROMOS96 manual and user guide, Zürich, Switzerland: Hochschulverlag AG an der ETH Zürich

[57] TingGuang S, Ming L, WeiZu C & CunXin W (2010) *Sci China Life Sci* 53, 620-630

[58] Hockney R W & Eastwood J W (1981) *Computer simulation using particles*, New York, McGraw-Hill

[59] Berendsen HJC, Postma JPM, DiNola A, Haak JR (1984) *J. Chem. Phys.* 81: 3684–3690

[60] Hess B, Bekker H, Berendsen H J C & Fraaije J G E M (1997) *J. Comp. Chem*. 18, 1463–1472

[61] Essmann U, Perera L, Berkowitz M L, Darden T, Lee H & Pedersen L G (1995) *J. Chem. Phys*.103, 8577–8592

[62] Voelz V A, Dill K A & Chorny I (2011) *Peptide Science* 96, 639-650

[63] Zi H F & Zang H X (2005) *J. Mol. Structure (Theochem)* 756, 109-112

[64] Jain A, Purohit C K, Verma S & Shankararamankrishnan R (2007) *The J. of Physical Chemistry B Letters* 111, 8680-8683

[65] Egli M & Sarkhel S (2007) *Acc. Chem. Res*. 40, 197-205

[66] Gautrot J E, Hodge P, Cupertino D & Helliwell M (2006) *New J. of Chemistry* 30, 1801-1807

[67] Maccallum P H, Poet R & Milner-White E J (1995) *J. Mol. Biol*. 48, 374-384

[68] Maccallum P H, Poet R & Milner-White E J (1995) *J. Mol. Biol*. 248, 361-373

[69] Allen F H, Baalham C A, Lommerse J P M & Raithby P R(1998) *Acta Crystallogr* B54, 320-329

[70] Allen F H, Dacies J E, Galloy J J, Johnson O, Kennard O, Macrae C F, Mitchell E M, Mitchell G F, Smith J M & Watson D G (1991) *J Chem Inf Comput Sci* 31, 187-204

[71] Deane C M, Allen F H, Taylor R & Blundell T L (1999) *Protein Engineering* 12, 1025-1028

[72] Nandel F S, Kaur H, Malik N, Shankar N & Jain D V S (2001) *Indian J. Biochem. Biophys*. 38, 417-425

[73] Nandel F S & Kaur H (2003) *Indian J. Biochem. Biophys*. 40, 265-273

[74] Nandel F S & Saini A (2011) *J. of Biophysical Chemistry* 2, 37-48

[75] Nandel F S, Jaswal R R, Saini A, Nandel V & Shafique M (2014) *Journal of Molecular Modeling* 20, 24-29

[76] Desiraju G R & Steiner T(1999) *The Weak Hydrogen Bond: In Structural Chemistry and Biology*, Oxford Science Publications

[77] Peggion E, Cosani A, Verdini A S, Del Pra A & Mammi M (1968) *Biopolymers* 6, 1477-1486

[78] Urry D W, Glicksan J D, Mayery D F & Haider J (1972) *Biochemistry* 11, 487-493

[79] Schuler B, Lipman E A, Steinbach P J, Kumke M & Eaton W A (2005) *Proc Natl Acad Sci USA* 102, 2754–2759

[80] Ungar-waron H, Gurari D, Hurwitz E & Sela M (1973) *Eur J Immunol* 3, 201–205

[81] Miranda L P & Alewood P (1999) *Proc. Natl. Acad. Sci. U.S.A.* 96, 1181-1186

[82] Sato S, Kwon Y, Kamisuki S, Srivastava N, Mao Q A, Kawazoe Y & Uesugi M (2007) *J Am Chem Soc* 129, 873–880

[83] Jitariu L C, Wilson C & Hirst D M (1997) *Journal of Molecular Structure (Theochem)* 391, 111-116.

[84] Schmid E D & Brodbek E (1985) *Can. J. Biophys*. 63, 1365-1371.